ANTENNA ARRAYS

Consisting of two to thousands of antenna elements, an array antenna presents the ultimate in flexible antenna pattern control. This capability includes electronic scanning, planar or conformable apertures, the ability to transmit or receive multiple shaped patterns, and adaptive control for jammers, clutter, and multipath suppression and for the reduction of cosite interference. Arrays benefit from technological advances, and they are the key technology drivers for solid state T/R (transmit/receive) modules, advanced signal processing, and photonic technology.

Antenna arrays are often simply called "phased" arrays, a term that refers to the progressive phase shift introduced to scan the beam. We will use this term throughout this section, although the beam can be scanned by either time delay devices or phase shifters, depending on the required system's bandwidth. The distinction will be addressed later.

The basic principle behind the operation of the phased array, as illustrated in Fig. 1, is that the RF power be divided among a number of elements by a power divider, with each element signal shifted appropriately in phase or in time. Relative time delay is portrayed in the sketch by circular phase fronts emanating from each element of the array, with signals either radiated at the same time [Fig. 1(a)] or delayed in time by an increasing amount from left to right so that the rightmost signal radiates last. The figure shows how radiation from each element adds in space so as to create an outgoing wave with an appropriate scan angle. Although not shown in the figure, the array power divider usually provides equal line lengths from the source to each element because this leads to optimum system bandwidth.

The power divider can also be used to control the signal amplitude at each element. This unequal power division is called amplitude "tapering," and it provides for sidelobe control. At broadside, with element spacing chosen properly, the array directivity is that of the broadside aperture,

$$D_B = \left(\frac{4\pi A}{\lambda^2}\right)\epsilon_a \qquad (1)$$

where A is the aperture area and ϵ_a is the aperture efficiency, which depends on the array's taper design. The scanned beam of Fig. 1(b) will have reduced directivity and (usually) additional losses that further reduce the array gain.

ARRAY ARCHITECTURE AND COMPONENTS

Figure 1 also indicates the basic components that make up a phased array. They consist of a power divider/combiner, phase shifters, and radiating elements. This simple sketch understates the tremendous number and variety of components that make up array technology, and it also understates the importance of an overriding array architecture aimed at satisfying the system needs. The following paragraphs will illustrate some of these issues.

Architecture is the *character and style of building* of a structure or system. The term *array architecture* implies that there are significant choices to be made in the design of an antenna array system; these choices can completely change the design, packaging, cost, and function of the system. The architecture of the system needs to be determined by the antenna system engineer working with the radar, communications, and avionics system engineers.

One type of an array may be an ideal solution for a requirement at, say, 12 GHz but altogether inappropriate at 120 GHz. The 12 GHz design may be a waveguide array with ferrite phase shifters, but at 120 GHz active solid state circuitry may have replaced the ferrite phase shifters, microstrip replaced the waveguide, patch radiators replaced the waveguide elements, and monolithic fabrication replaced the machined part fabrication. These two arrays will therefore have completely different architectures.

This section will describe some of these components and illustrate the interdependence of system architecture and component selection.

Power Dividers

Selecting the way RF power is combined or distributed within the array is a major architectural choice. Constrained (or often termed *corporate*) power divider networks can be fabricated using waveguide, coaxial line, stripline, or any of the various printed circuit transmission media like microstrip, slot line, and others. Aside from the choice of transmission medium, the most important choice is the selection of an organization for the aperture. Many arrays use a power divider network with as many ports as antenna elements. This is a very simple organization, with one array element excited from each port of the power divider. Amplitude illumination (taper) is provided by the power divider or occasionally by adding loss at the element level. The array is then assembled one element at a time, with elements supported by the power divider itself. Cost reductions have come from grouping elements of the array into *subarrays*; that are readily mass-produced and that incorporate necessary bias and logic circuitry as well as RF power division. Figure 2 shows two basic ways of constructing the aperture. Figure 2(a) shows an array of column subarrays assembled using *brick* construction in which the power divider network, in addition to all the phase shifters and sometimes the antenna element, are constructed on a single panel. The distinguishing feature of brick construction is that the array elements are at the panel's edge. The panel is then inserted into the array as a brick into a wall. Figure 2(b) shows an array made up of area subarrays called *tiles*. Tiles tend to be multilayer geometries with the power divider network and elements occupying different layers in the same tile. The tiles are placed side by side to build the array. These fundamentally different organizations dictate (and in turn are dictated by) the selection of solid-state components, circuitry, and the array elements.

In addition to such constrained networks, a number of arrays are built using space feeds, wherein a horn antenna illuminates the back or front face of an array to provide power division. Space-fed arrays are more bulky then corporate-fed arrays, but they are usually far less expen-

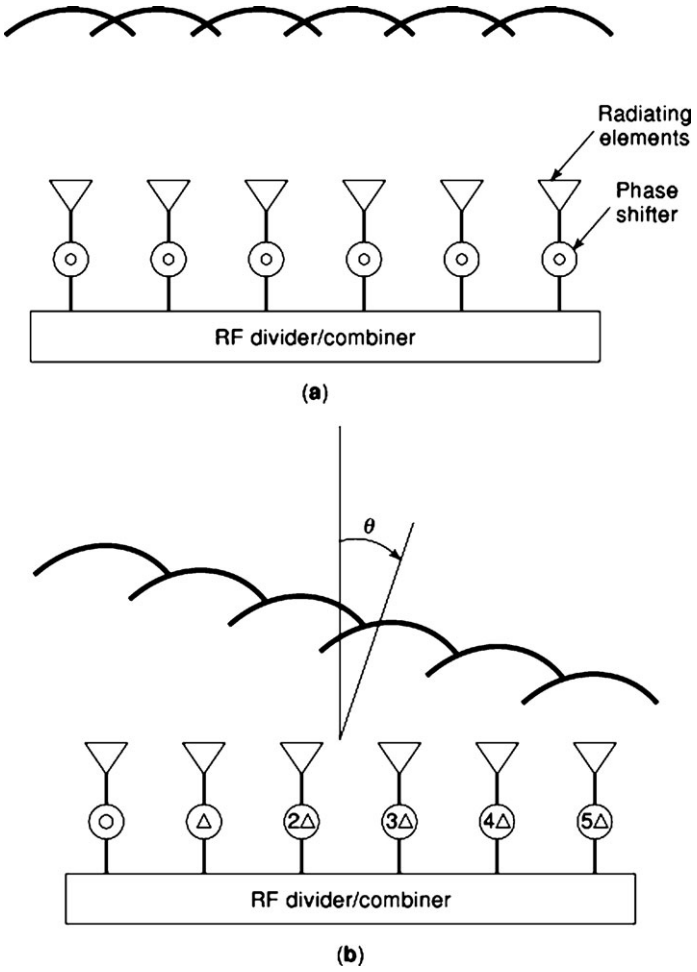

Figure 1. Radiation from antenna arrays. (a) Array radiating broadside. (b) Array radiating to angle θ.

sive and often lighter. Figure 3(a) shows that with one such space feed, the array is used as an active lens. Array elements at the back face of the array receive the RF power from the horn feed. Phase shifters installed in the path between array back and front faces correct for the nearly spherical wavefront of the incident wave and then add the progressive phase distribution to scan the beam. Figure 3(b) shows the reflectarray concept in which the array is space-fed from the front. Again the elements at the front face of the array receive the distributed power, and phase shifters provide the necessary phase correction and scanning control. The back face of the array is short-circuited, so the RF signal goes through the phase shifter twice before it radiates. This tends to make reflectarrays somewhat more lossy and the phase shifter more tolerance sensitive than lens arrays. This feature, and undesirable feed blockage as indicated in Fig. 3(b), for low-angle radiation have made space-fed lens arrays the more popular choice for most space-fed systems.

Phase Shifters and Time Delay Units

Phase shifters are devices that change the phase of a signal traveling down the feed transmission line. Usually the devices have discrete phase states, so one measure of the quality of the phase shifter is the number of *bits*, or digital states, by which it approximates a continuous phase distribution from zero to 360 degrees. For example, an n-bit phase shifter has n different phase states that are used in cascade; it can produce 2^n different output phases. A three-bit phase shifter consists of a 180-degree state, a 90-degree state, and a 45-degree state. Starting at zero phase and switching in various combinations produces 2^3 or 8 output phases from 0 to 315 degrees at 45-degree intervals. The 360-degree output phase is the same as 0-degree phase, so clearly all the required phases are produced with the three cascaded bits.

Current phase shifters use either ferrite material in the transmission lines, with propagation constants changed by electrical currents, or diode-loaded circuits, which are embedded in the transmission line network. Figure 4(a) shows a ferrite torroid phase shifter in a waveguide configuration. The phase shift state is selected by passing a current pulse of calibrated duration and amplitude through the ferrite core. This is only one of a number of useful ferrite phase shifter types, and a more complete listing can be found (1) in the literature. Typically ferrite phase shifters can provide extremely precise phase shift, insertion loss less than 1 dB, and can handle hundreds of watts of average power.

Figure 4(b) shows one section of a switched line phase shifter that inserts an effective path length l_1 or l_2, depending upon the settings of switches s_1 and s_2. Diodes can also be used to switch much longer lengths of line and so can

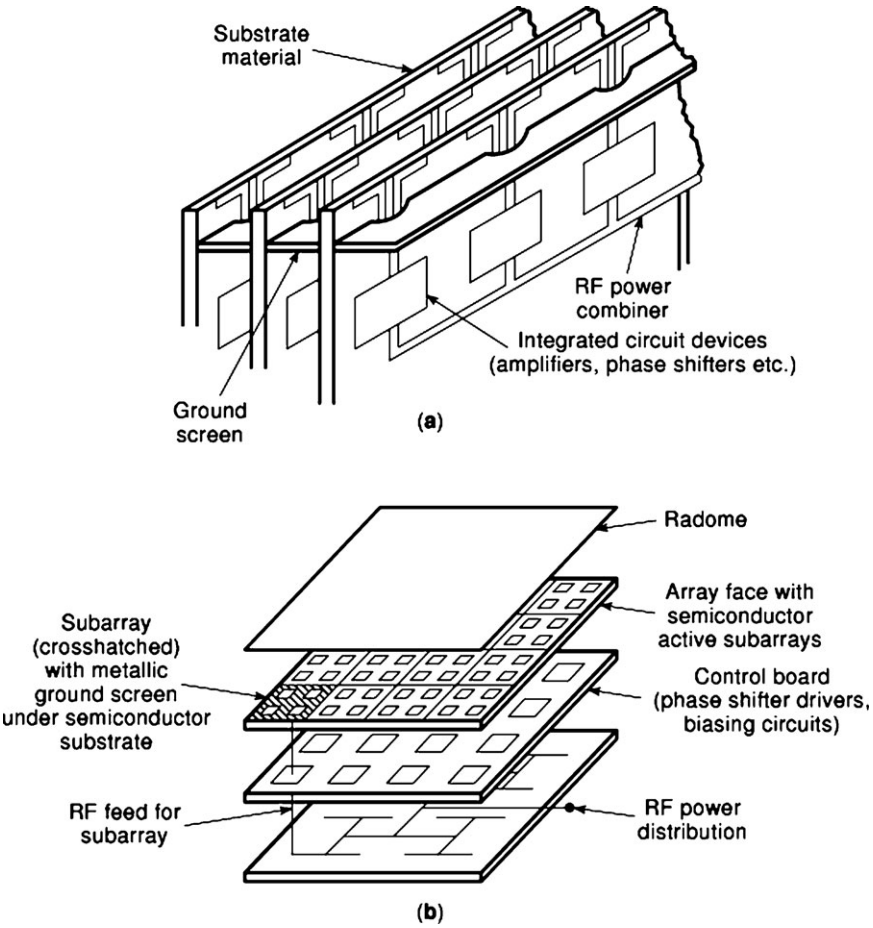

Figure 2. Array and subarray configurations. (a) Column subarrays with brick construction. (b) Area subarrays with tile construction.

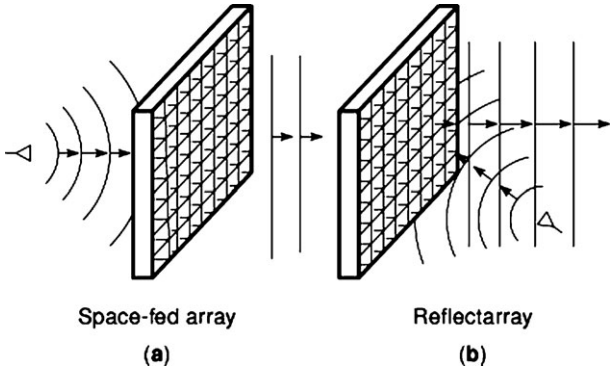

Figure 3. Space fed arrays. (a) Lens array. (b) Reflectarray.

be used to control time delay devices. In a phase shifter, the added sections of line are all a fraction of a wavelength long, so that the longest electrical path difference through the device is, as described earlier, one bit less than 360 degrees longer than the shortest path. A time delay device, however, needs to represent many wavelengths of delay, and it in fact needs to insert lengths of line comparable to the physical length of the array. Such devices are often lossy, complex, bulky, and costly but may be essential for wideband array performance depending on array size and scan requirements.

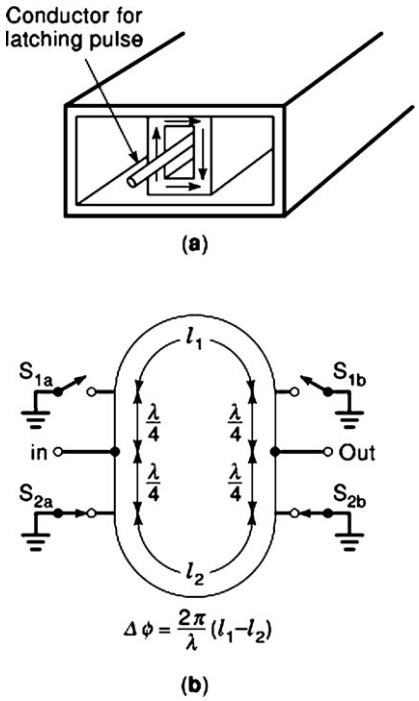

Figure 4. Phase control devices. (a) Ferrite phase shifter. (b) Diode switched line phase shifter.

The switched line phase shifter is only one of many solid-state phase shifter designs. Some phase shifters use a switched line section for one or several of the smaller bits but hybrid circuits or loaded line circuits for the larger bits. These and other circuits are sometimes less frequency dependent, require fewer diodes, or occupy less space than the switched line type. Sharma (2) gives an accounting of the state of the art in solid-state phase control devices.

Array Elements

The final, and most important, array component is the radiating element itself. The element determines the ultimate bandwidth, polarization, weight, and cost of the entire radiating system in addition to fundamental architectural issues like integration with the transmission medium and the choice of distributed solid-state power modules or central tube source. Practical radiating elements range from open-ended waveguides to dipoles or monopoles and a variety of printed elements coupled to the transmission medium. Figure 5(a–c) shows elements used for tile fabrication, while Fig. 5(d–e) shows elements for brick construction. The microstrip patch-fed tile element of Fig. 5(a) is simple to fabricate and can be fed on-line or by using probe feeds, or aperture coupled from a lower-layer circuit, but has only a few percent signal bandwidth in the array environment. The proximity coupled patch element of Fig. 5(b) can have bandwidth exceeding 10%. Strip-line-fed cavity-backed slots as shown in Fig. 5(c), can be much wider bandwidth, but they are difficult to fabricate because of the need to define the cavities using plated holes. The elements for brick construction are typically wider band but do protrude from the aperture. Over modest scan sectors, stripline dipoles [Fig. 5(d)] can have up to 40% bandwidth, while flared notch elements [Fig. 5(e)] can have up to 4:1 bandwidth.

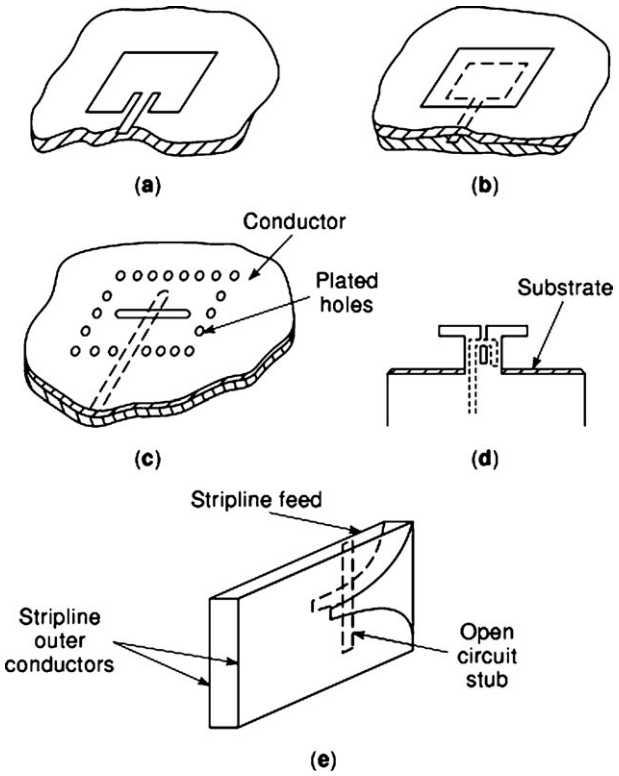

Figure 5. Array elements. (a) Microstrip patch element. (b) Proximity coupled microstrip element. (c) Stripline fed cavity backed slot element. (d) Strip line fed dipole element. (e) Flared notch element fed by stripline center conductor.

ARRAY THEORY

Array Antenna Patterns

The far-field pattern of an array of N elements in the generalized geometry of Fig. 6 can be written in terms of the incident transmission line voltage signals a_n and the element locations $\bar{r}_n$ as

$$\boldsymbol{E}(\theta,\phi) = \frac{e^{-jkR_0}}{R_0}\sum_{n=1}^{N} a_n f_n(\theta,\phi) e^{j\bar{k}\cdot\bar{r}_n} \qquad (2)$$

for

$$\bar{r}_n = \hat{x}x_n + \hat{y}y_n + \hat{z}z_n$$
$$\bar{k} = \hat{x}k_x + \hat{y}k_y + \hat{z}k_z$$

where $k_x = ku$, $k_y = kv$, $k_z = k\cos\theta$, and $k = 2\pi/\lambda$.

The parameters $u = \sin\theta\cos\phi$; $v = \sin\theta\sin\phi$ are called *direction cosines* of the angular location (θ, ϕ). The use of the direction cosine parameters u and v greatly simplifies the evaluation of beamwidth, bandwidth, and scanning parameters, so they are routinely used in array analysis.

In these expressions, $\bar{k}$ is the vector wave number or propagation constant of a plane wave radiating in the direction of (θ, ϕ) and $k = 2\pi/\lambda$ at wavelength λ. $f_n(\theta, \phi)$ is the far-field pattern of that nth element in the array environment.

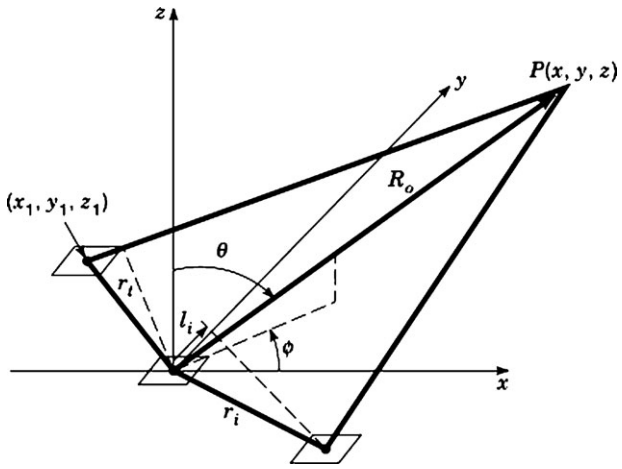

Figure 6. Generalized array configuration.

The multiplying factor $\exp(-jkR_0)/R_0$ is common to all expressions, and it will be suppressed hereafter. In this expression we have assumed each element to have a single input port, but an obvious generalization would include additional ports by including additional $a_n f_n$ terms. Finally, the above summation applies for generalized array of any dimensionality and conforming to any surface.

In general, the element patterns $f_n(\theta, \phi)$ are different for each array element even though all the elements are the same. These differences occur because each element pattern includes the scattered radiation from all other elements, from the array edges, and any other scattering from the mounting structure. Element pattern differences due to element interaction will be discussed later. In the special case of array elements mounted conformal to some nonplanar body, like a rocket or aircraft nose radome, the elements do not even point in the same direction, so the element patterns are fundamentally different in this case.

Before discussing the general cases, let us consider a linear array of elements located in a plane at x_n with $y_n = z_n = 0$ but otherwise arbitrarily spaced in the x direction:

$$\boldsymbol{E}(\theta, \phi) = \sum_{n=1}^{N} a_n f_n(\theta, \phi) e^{jkx_n u} \tag{3}$$

If all of the element patterns $f_n(\theta, \phi)$ are the same [and given by $f(\theta, \phi)$], then the expression becomes

$$\boldsymbol{E}(\theta, \phi) = f(\theta, \phi) \sum_{n=1}^{N} a_n e^{jkx_n u} \tag{4}$$

When this separation can be made, the pattern is expressed as the product of an element pattern $f(\theta, \phi)$ and an array factor (the indicated summation).

NARROWBAND AND WIDEBAND SCANNING

Consider the plane $\phi = 0$ for convenience. This expression [Eq. (5)] can have a maximum at different angles depending on the choice of a_n. To move a principal maximum to some angle θ_0 at a single frequency ($\lambda = \lambda_0$), the required phased element excitations are given by:

$$a_n = |a_n| e^{-jk_0 x_n u_0} \tag{5}$$

for $k_0 = 2\pi/\lambda_0$ and $u_0 = \sin\theta_0$. Substituting Eq. (6) into Eq. (5) results in:

$$\boldsymbol{E}(\theta, \phi) = f(\theta, \phi) \sum_{n=1}^{N} a_n e^{j2\pi\left(\frac{u}{\lambda} - \frac{u_0}{\lambda_0}\right)x_n} \tag{6}$$

The pattern has a maximum value at $u = u_0$ ($\theta = \theta_0$ in the plane $\phi = 0$) when $\lambda = \lambda_0$. However, for a signal at some other frequency, since phase shifters produce a phase change that is nearly independent of frequency, Eq. (7) shows a peak at the angle θ whose sine is

$$\sin\theta = \left(\frac{\lambda}{\lambda_0}\right) \sin\theta_0 \tag{7}$$

This beam angle moves, or squints, as a function of frequency as indicated in Fig. 7, with the beam peak farthest from broadside at the lowest frequency and nearest to broadside for the highest frequency.

This squint angle change can be interpreted in terms of a fractional bandwidth by assuming an array beamwidth of Δu and assuming that the beam is placed exactly at the angle θ_0 at center frequency f_0. Then defining the upper and lower usable frequencies to be those at which the gain is reduced to half at the angle θ_0 results in the fractional bandwidth

$$\frac{\Delta f}{f_0} = \frac{\Delta u}{\sin\theta_0} \tag{8}$$

Arrays with narrow beamwidths thus have less bandwidth, and inverse proportionally less bandwidth as the scan angle is increased.

If true time delay devices were used to collimate the beam, the available excitation would take the form

$$a_n = |a_n| e^{-jkx_n u_0} \tag{9}$$

In this expression the wave number k is the same as that used in Eq. (5), and it varies linearly with frequency. With this excitation the far-field radiation will always have its peak at u_0 for all frequencies, and the array bandwidth is only limited by device operation, not pattern squint. This state is highly desirable, but true time delay devices are costly, lossy, and can constitute a major architectural issue in the design of arrays systems.

Periodic Arrays and Element Spacing

Most phased arrays consist of elements placed in a one- or two-dimensional planar grid with equal element spacings. There are several advantages in doing this. First, the periodic grid allows very precise pattern formation. Second, both the fabrication and array excitation are simplified by using the periodic arrangement of elements. However, the periodicity also imposes constraints on element spacing in order to avoid the formation of unwanted radiation peaks, called *grating lobes*.

The grating lobe phenomenon is apparent from an inspection of Eq. (11) below. Consider the one-dimensional array with elements at the locations $x_n = nd_x$ and operating at the single frequency λ_0 scanned by phase shifters. In the plane $\phi = 0$ the pattern given by Eq. (7) becomes

$$\boldsymbol{E}(\theta, \phi) = f(\theta, \phi) \sum_{n=1}^{N} |a_n| e^{jk_0 nd_x(\sin\theta - \sin\theta_0)} \tag{10}$$

The summation has its maximum when the exponent is zero for all n. This is the peak of the main beam of the array, but it is also maximum when the exponent is any multiple p times $2\pi n$. At these peaks, or grating lobes, the radiation is as large as it is at the main beam location ($\theta = \theta_0$). These grating lobe angles are given by the angles θ_p for which

$$\sin\theta_p = \sin\theta_0 + \frac{p\lambda_0}{d_x} \tag{11}$$

for

$$\sin|\theta_p| \leq 1$$

for p all positive and negative integers. Angles described by $\sin|\theta_p| > 1$ do not correspond to real angles, so they are often referred to as being in *imaginary space*.

Figure 8 shows the array factor of two linear arrays scanned to 45° ($u_0 = 0.707$). The first array, with pattern shown solid, has 64 elements with $\lambda_0/2$ spacing, and the second has 16 elements with $2\lambda_0$ spacing. Both patterns

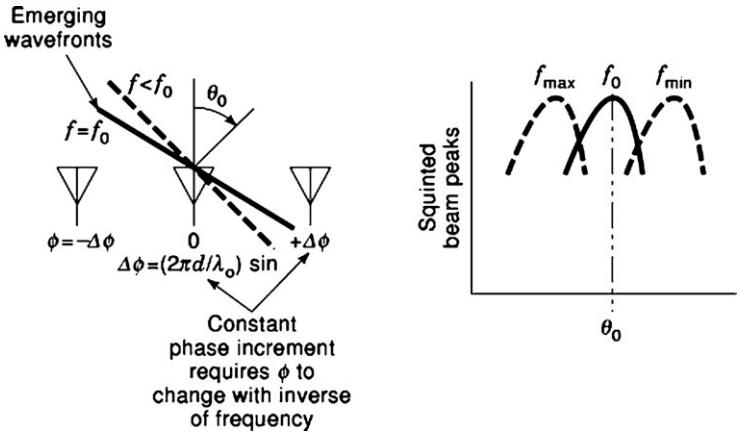

Figure 7. Array beam squint for phase steered array.

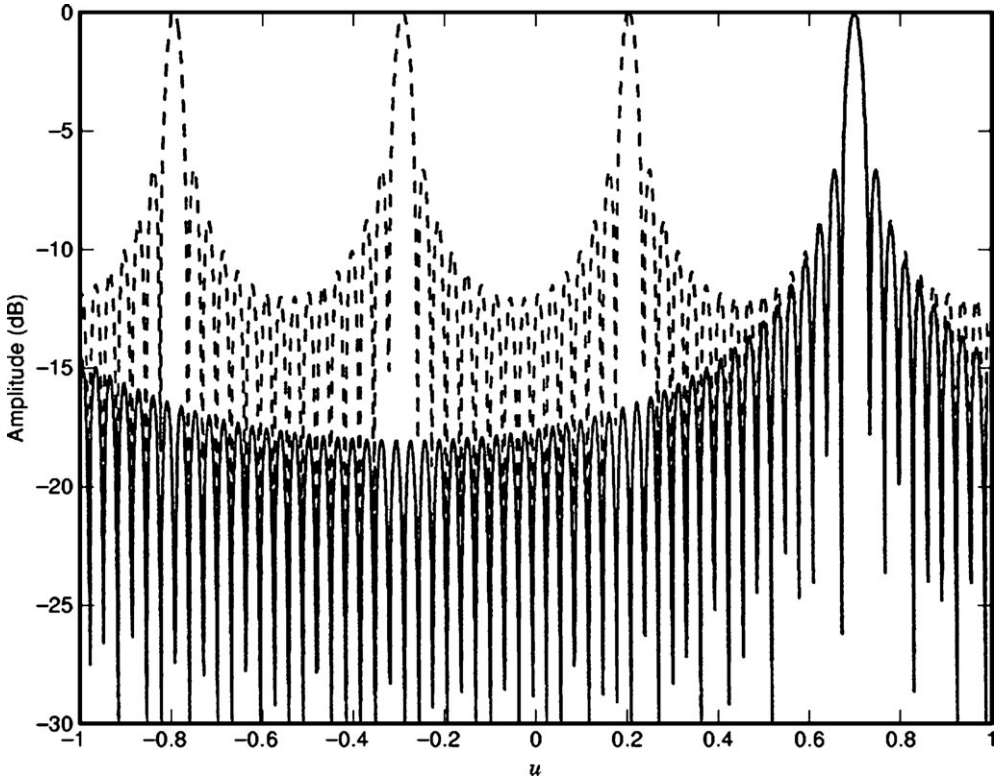

Figure 8. Array factors illustrating grating lobe phenomenon. Solid curve: column array of 64 half wavelength spaced elements scanned to 45 degrees. Dashed curve: column array of 16 elements with 2 wavelength spacing.

peak at the scan angle, but the envelope of the pattern of the array with half-wave-spaced elements falls monotonically away from that angle until it reaches a minimum at $u = -0.293$ that is half way to a suppressed grating lobe at $u = -1.293$ (in imaginary space). The dashed pattern additionally has grating lobes at multiples of 0.5 from the peak, and a number of them exist and radiate in real space.

Equation (12) also leads to an expression for the largest spacing allowable for any array that scans to some given angle. Since only values of $\sin\theta$ between zero and ± 1 represent real angles, the array spacing must be such that for any scan angle u_0 none of the grating lobes enters the region $|\sin\theta| \leq 1$. This results in the constraint on spacing of

$$\frac{d_x}{\lambda_0} \leq \frac{1}{1 + \sin\theta_0 + u_3/2} \tag{12}$$

for u_3, the beam width between nulls of the array factor. Typically the beam width u_3 is on the order of $2\lambda_0/L$ for an array of length L.

Similar grating lobes are present in two-dimensional scanning arrays. A planar two-dimensional array with $M \times N$ elements on a rectangular lattice, $x_m = md_x$ and $y_n = nd_y$, scanned to angles θ_0 and ϕ_0 represented by the direction

cosines u_0 and v_0 has an array factor

$$F(u,v) = \sum_{m=1}^{M}\sum_{n=1}^{N} |a_{mn}| e^{jk_0[(u-u_0)md_x + (v-v_0)nd_y]} \qquad (13)$$

and has grating lobes u_p, v_q,

$$u_p = u_0 + \frac{p\lambda_0}{d_x} \qquad (14)$$

$$v_q = v_0 + \frac{q\lambda_0}{d_y} \qquad (15)$$

subject to

$$u_p^2 + v_q^2 \le 1 \qquad (16)$$

This equation places similar constraints on d_x and d_y as in the one-dimensional array.

Array Mutual Coupling

The previous section assumed that every element in the array radiated with the same element pattern. In fact an element in an array does not radiate the same pattern as if it were radiating in an isolated environment, nor does it present the same impedance or support the same current or field distribution. These effects are all evidence of a phenomenon called *mutual coupling,* depicted in Fig. 9(a), by which every element of the array interacts or couples with every other element. In the general case even the shape of the current distribution on each element changes with scan angle, and one must use a higher-order current approximation to evaluate the total radiation for each angle in space. Between these two limits, one assuming no interaction and one assuming fine scale changes with the scan angle, is the case where one can speak of single-mode elements and single-mode mutual coupling.

The solution of the general array mutual coupling problem involves a complex integral equation formulation and numerical solution. The solution is expressed in terms of a series of basis functions (possibly the harmonics in a Fourier series distribution) used to approximate the total current or aperture field. For the purpose of this discussion, it is convenient to think of these basis functions as modes and to consider the case where a single mode is a good representation for the current distribution on each antenna. This is often a good approximation because most array elements are small compared to a wavelength, and all element currents or fields are often nearly the same.

This one-mode assumption makes it simpler to explain the two complementary views of array mutual coupling. We will call these the mutual impedance viewpoint and the element pattern viewpoint.

From the mutual impedance perspective, we assume the single mode radiates with a pattern $f(u, v)$, which might be a vector quantity. Each transmission line excites an element that radiates into all other transmission lines through their elements, as indicated in Fig. 9(a). For an N element array on some nth element, the radiating field or current, here called I_n, is related to an input voltage matrix for the whole array by the square $N \times N$ impedance matrix Z ($V = ZI$). The I_n are unknown, so to compute the

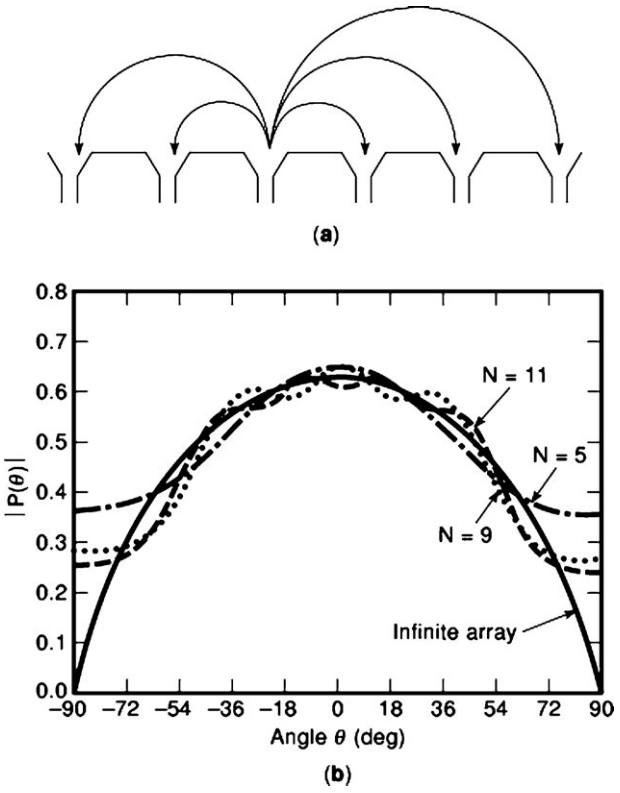

Figure 9. Array mutual coupling. (a) Coupling between array elements. (b) Element pattern $P(\theta)$ and reflection coefficient magnitude R of center element of unloaded waveguide array (B/λ = a/λ = 0.4) after Wu (3).

array radiation, one needs to invert the impedance matrix that relates the applied signals V_m to the produced I_n:

$$I = Z^{-1}V \qquad (17)$$

In summary, from this perspective one can find the array radiation from the applied sources by solving for the actual currents (or fields) that result. It turns out that the common problem of synthesizing a desired radiation pattern is handled by solving for the desired current and then using the impedance matrix to find the necessary applied sources.

The alternative point of view is focused on the array "element patterns" that radiate when each element is excited separately, with all other elements terminated in a matched load. When only one transmission line is excited, the total pattern is generated as the sum of contributions from all the element radiation. Consider a small aperture element that supports a single mode of field with radiation pattern $f(u, v)$. If that nth element alone were to radiate when excited by an incident signal a_n from the nth transmission line, then the radiation pattern of that element would be $a_n e(u, v) e^{-j\bar{k}\cdot \hat{x}^x{}_n}$. The exponential term is due to the location of the element in the array. However, as indicated in Fig. 9(a), that element scatters its radiation into every other element, inducing a field on any m'th element that is given mn'th term of the scattering matrix S. The total radiation from the array with one element excited is

thus:

$$E_n = a_n f(u, v)\left(e^{-j\vec{k}\cdot\hat{x}x_n} + \sum_{m=1}^{N} S_{mn} e^{-j\vec{k}\cdot\hat{x}x_m}\right) \qquad (18)$$
$$= A_n f_n(u, v) e^{-j\vec{k}\cdot\hat{x}x_n}$$

where

$$f_n(u, v) = f(u, v)\left[S_{nn} + \sum_{m=1}^{N} S_{mn} e^{-j\vec{k}\cdot\hat{x}(x_m - x_n)}\right]$$

This expression shows the radiation to consist of a primary radiation from the excited element, plus a scattered term given by S_{nn} times the primary term, plus terms S_{mn} times the primary term but radiating from the location of the other elements (x_m). From this perspective each element radiates with a different element pattern $f_n(u, v)$because each element pattern contains radiation from every element of the array. The total radiation is the sum of all these element patterns weighted by the incident transmission line signals. Figure 9(b) shows an example (3) of the element pattern of an isolated antenna element and the same element in an array. This figure shows the element pattern of the center element of an array of N waveguide elements for $N = 5, 9, 11$ and an infinite array. The figure shows the effect of mutual coupling on element pattern as resulting in periodic ripples with higher periodicity for longer arrays and that the end-fire gain ($\theta_0 = \pm 90$ degrees) reduces because of coupling until it is zero for the infinite array case. One can show that the optimum gain varies like $\cos\theta$ for the infinite case.

Beam Broadening and Directivity Loss with Scan

The expressions for the scanned array pattern indicate that for constant frequency f_0, either phase shifters or time delay units form a beam with peak at the scan parameters (u_0, v_0) and that the shape of that pattern only depends on the displacement $(u - u_0, v - v_0)$ and not the scan parameters. The pattern is displaced with scan and otherwise remains unchanged. The array beam width is therefore constant in (u, v) space for any given azimuth angle ϕ, but in terms of the θ dependence, the beam width broadens as the array is scanned from zenith ($\theta = 0$) to the horizon. For a large array and scan angle θ_0 not too near the horizon, this beam width is given in terms of the beam width θ_B at broadside as

$$\Delta\theta = \frac{\theta_B}{\cos\theta_0} \qquad (19)$$

The beam width along the scan plane θ thus broadens like $\sec\theta_0$ as the array is scanned in θ.

Accompanying this beam width increase is a decrease in array directivity so that the directivity is given in terms of the broadside directivity D_B as

$$D_0 = D_B \cos\theta_0 \qquad (20)$$

ARRAY SYNTHESIS

Many useful pattern synthesis techniques for planar or linear antenna arrays follow directly from existing methods developed for aperture or continuous one-dimensional antennas. This is so for several reasons. First, as long as the elements are closely spaced and grating lobes well out of the radiating region, the array periodicity does not significantly alter the pattern structure. Second, the distinctions that do exist come from the mutual coupling and are evident in array edge effects, or equivalently from the observed different element patterns across the array. As long as the elements support only the single-mode fields, these issues do not alter the synthesis procedure, since one can synthesize in terms of the currents and aperture fields that create radiation, or in terms of the measured or computed array element patterns, and then include mutual coupling to evaluate the necessary applied excitation.

The basis for most aperture synthesis is the Fourier transform relationship between aperture field and far field for a continuous aperture. If the arrays are large and the elements closely spaced, this procedure is not sensitive to the discretization or edge effects, and the method is quite accurate. The transform method is also especially convenient because of its application to arrays that are not periodic and for arrays conformal to gently curved geometries.

Arrays periodic in one or two dimensions have far-field patterns describable by discrete Fourier transform pairs. In one dimension the array factor at wavelength λ is written

$$F(u) = \sum_{n=1}^{N} a_n e^{jknd_x u} \qquad (21)$$

where the sum is taken symmetrically about the array center. The coefficients a_n are the array element excitation and are given from orthogonality as

$$a_n = \frac{d_x}{\lambda}\int_{-\lambda d_x/2}^{\lambda d_x/2} F(u) e^{-jkund_x}\, du \qquad (22)$$

In this expression the integral is taken over the periodic distance in u space, namely half way to the two nearest grating lobes for a broadside beam. Used in this way, the technique gives the best mean square approximation to the desired pattern. This feature is lost if spacings are less than half wavelength, although the technique is still useful.

A second technique that has found extensive application is the "Woodward" synthesis method (4). This approach uses an orthogonal set of pencil beams to synthesize the desired pattern. The technique has important practical utility because the constituant orthogonal beams are naturally formed by a Butler (5) matrix or other multiple-beam system.

Other techniques for periodic arrays are based on the polynomial structure of the far-field patterns. These include the method of Schelkunov (6), the Dolph-Chebyshev method (7), and others. Among the most successful and used methods are the pencil beam synthesis technique of Taylor (8) and the associated monopulse syntheses technique of Bayliss (9). These techniques are derived

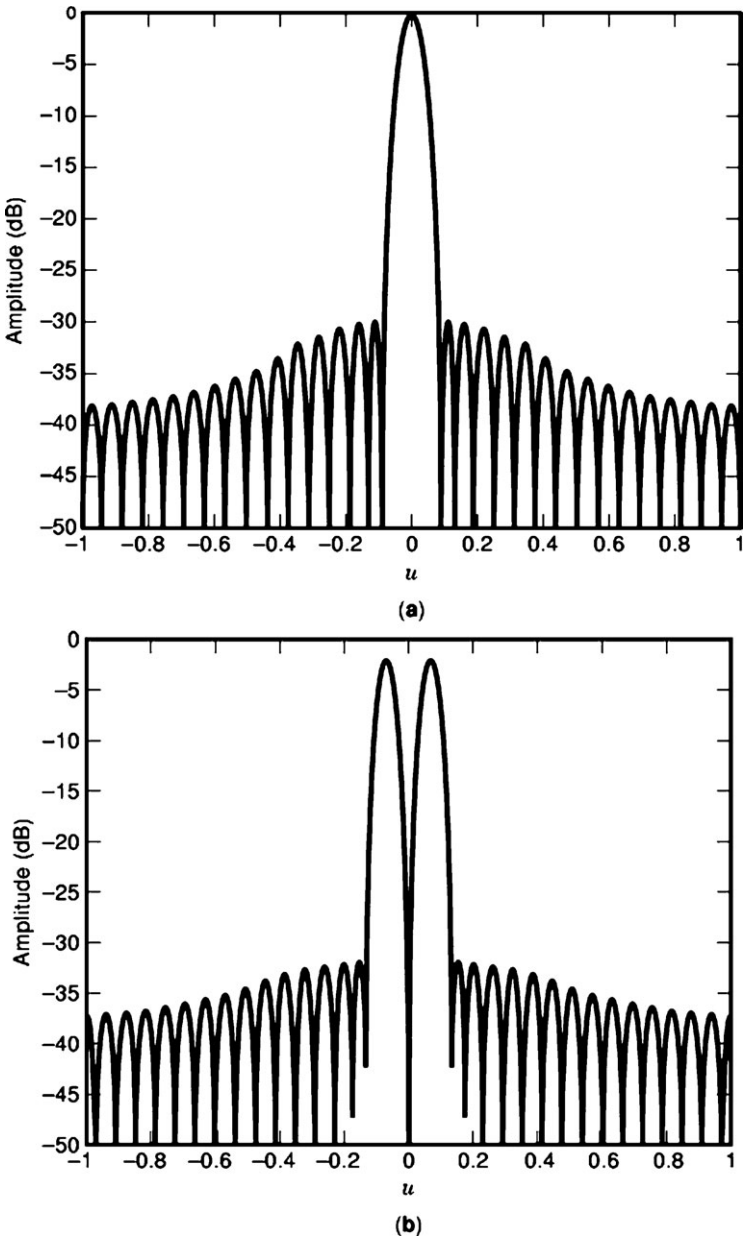

Figure 10. Low sidelobe sum and difference pattern synthesis. (a) Taylor sum pattern with −30 dB ($\bar{n}$ = 6) pattern. (b) Bayliss difference pattern with −30 dB ($\bar{n}$ = 6) pattern.

as improvements to the equal ripple method of Dolph-Chebyshev, and result in more realizable aperture distributions, improved gain and other advantages. Figure 10(a–b) shows the array factors for 32 element arrays with 30 dB Taylor and Bayliss distributions. Note that the first sidelobe in both cases is very close to −30 dB with respect to the pattern maximum. In general, the discretizing of continuous distributions introduces errors in the synthesized pattern, and these are more significant for small arrays or for arrays that are forced to have very low sidelobes. Space precludes giving a detailed description of these procedures, but they are described in detail in a number of references. Usually discretizing the continuous distribution is not a problem, but when it is, there are a number of iterative techniques to converge to the original desired pattern. Notable among these is the work of Elliott (10).

Finally, in addition to these classic synthesis procedures, there have been many iterative numerical solutions to the synthesis problem. These have, in general, been shown to be efficient and useful. One successful iterative procedure was introduced by Orchard (11) that allows for complete power pattern design, even to the extent of controlling each pattern ripple or sidelobe level. Other recently developed methods have used simulated annealing or genetic algorithms (12).

Aperiodic and Conformal Arrays

Aperiodic Arrays. A periodic array that fully occupies an entire aperture has several advantages. The directivity of such a uniform array at broadside is that of the filled aperture, namely $4\pi A/\lambda^2$ for an array with aperture area A. In addition the pattern (neglecting errors) can have very low sidelobes as long as spacings are chosen small enough

to eliminate grating lobes. However, there are times when (usually for economy) one chooses to populate an aperture with fewer elements. This procedure, called *thinning*, results in an array with nearly the full aperture beam width but using only a fraction of the elements in the filled array. If this thinning were done by simply increasing the element spacing of a periodic array, then the resulting pattern would have many undesired grating lobes. In the limit it would take on an interferometerlike pattern.

Instead, in many thinned arrays, elements are placed at randomized locations, whether on a rectangular grid or not, and often excited with uniform illumination. With thinned arrays the structured sidelobes can be lowered by tapering the density of excited antenna elements, instead of the aperture power, as done for a filled aperture. This is done (13) by selecting element locations statistically and choosing element weights as unity or zero with probabilities either equal to or proportional to the filled-array taper. The proportionality constant K is unity if the one/zero probability is chosen equal to the array taper ratio. At $K = 1$ the array is fully populated near the center, where the array taper is nearly unity. If K is chosen less than unity, then the array is not fully populated at the center, but the thinning is still proportional to taper. Since the algorithm is a statistical process, the resulting aperture illumination and pattern are not unique, but one can describe the average of the ensemble of arrays constructed from the algorithm. For this ensemble one can show that the resulting average pattern is the sum of two patterns, one of which is the ideal pattern of the filled, tapered array, multiplied by the number K. The second pattern is the average sidelobe level, a constant value with no angle dependence. For a large, highly thinned array the average sidelobe level is approximately $1/N_r$, normalized relative to the pattern peak, where N_r is the number of remaining elements. The average directivity is approximately N_r times the directivity of an element pattern. The reason for this result is that all signals add linearly at the beam peak, but elsewhere in the pattern they combine like the average of a random process. For this reason the normalized average sidelobe level is at the level of isotropic radiation, or the factor N_r below the peak directivity. Figure 11 shows a thinned array resulting from using the above algorithm directly. The dashes shown in the figure indicate elements left out of the square, half wavelength, lattice of a 25 wavelength radius aperture. The selected ideal pattern for the filled array is a 50 dB Taylor pattern [Fig. 11(b)] and it is approximated with 7845 elements excited. Given this number of elements, the average sidelobe level is about 39 dB, and this is about what is indicated in the Fig. 11(c). Nearly one hundred thousand elements would be needed to produce the 50 dB pattern desired, so clearly thinned arrays do not satisfy most low sidelobe array requirements. They do, however, present the least expensive way to provide very narrow beam width wide-angle-scanned patterns with moderate sidelobes.

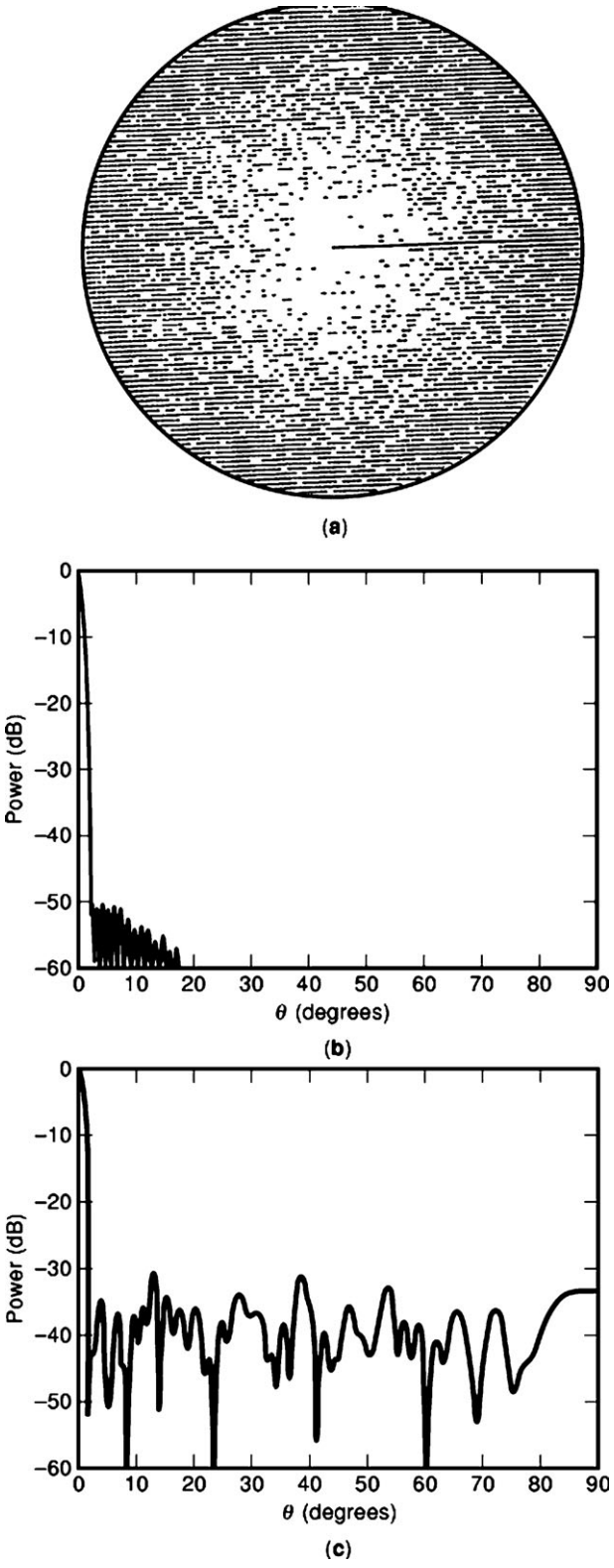

Figure 11. Circular array with elements removed). (a) Geometry (dashes show elements removed. (b) Desired Taylor pattern of filled array. (c) Pattern of thinned array.

Conformal Arrays. Conformal arrays are a special class of antennas that are built to conform to the surface of some vehicle, like an aircraft, spacecraft, missile, ship, or even an automobile. Depending on the array size and the local radius of curvature, this can pose a significant problem to the

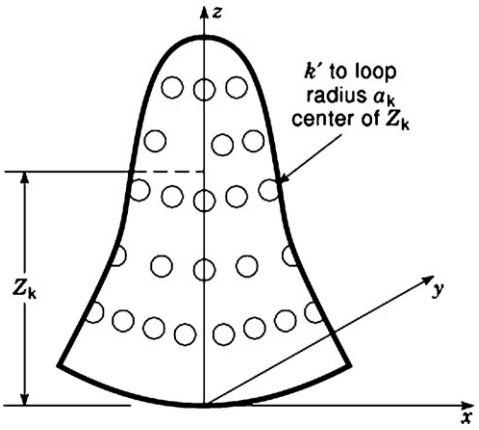

Figure 12. Generalized array conformed to a body of revolution.

practical realization of any desired pattern. The primary technical challenge is that the elements point in different directions, so the control network needs to provide variable amplitude and phase weighting to scan the array. An extreme but very important example is the use of an array on a cylindrical surface like that of the vehicle shown in Fig. 12 for scanning over a hemisphere. When a beam radiates in one direction, it is necessary to commute the amplitude distribution around the cylinder in order to avoid radiating energy into undesired regions. Many elaborate networks have been designed for performing this commutation, but it remains an expensive process requiring sophisticated design and packaging concepts.

Not all conformal arrays are mounted in such severely curved shapes as to require signal commutation. Most conformal applications are for flush mounted or very low profile arrays on gently curved surfaces where the challenges are far less severe. Future applications include airborne arrays for satcom and aircraft to earth coverage, missile antennas, and a whole variety of commercial vehicle applications. Conformal arrays will continue to be a major growth area for array antennas.

TRENDS IN ARRAY ANTENNA DEVELOPMENT

Cost reduction, coupled with increasing capability, have led to major new applications for array technology. Array production costs have declined with advances in microwave solid-state components and circuits and with the development of printed circuit elements. Arrays with modest performance can now satisfy an increasing number of system needs. Alternatively, array antennas offer immense growth potential at the high end of performance capability. Though not inexpensive, a variety of very high performance arrays provide for multifunction capability and pattern features like very low sidelobes or adaptive pattern control for clutter and jammer suppression. This capability is available using digital pattern control, where the phase shift or time delay functions are performed by digital sampling the RF or baseband signal and processing the N array outputs to do all adaptive and deterministic signal processing. Optically controlled arrays with fiber optic switched delay lines and other features provided by optical technology have

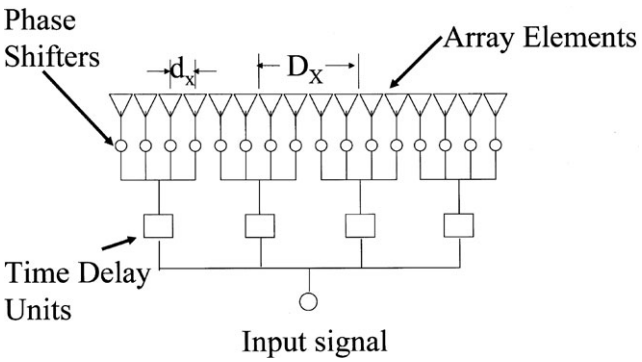

Figure 13. Array with phased elements and time-delay applied at the input to contiguous subarrays.

been built in laboratory models, and will play a role in providing ultrawideband multifunctional arrays.

Conformality and flexible control are the two features unique to array antennas, and the number of new applications continues to increase to fill demands in the two areas. Conformal scanning arrays provide high-gain antenna coverage from complex platforms, and when combined with elements of the increased flexibility, arrays will become especially good candidates for commercial applications such as in wireless communications and automotive radar. As the cost of solid-state modules continues to decrease, more applications will be filled by this "high-end" antenna technology.

Time Delay for Wide Band Arrays:

The phenomenon of phased array "squint" as described in equation 9 and Figure 7, is the primary factor limiting the instantaneous bandwidth of large phase steered arrays. There is no squint if time delay units can be used at every element, but for very large arrays this option may be far too costly. The practical, although band limiting, solution is to group elements into phase steered subarrays and then provide time delay behind each subarray. Figure 13 depicts an array of linear subarrays with time delay at each subarray input port, and phase shift across each 4-element subarray.

Figure 14 shows the behavior of an array of 8-element linear array subarrays. The array has 16 subarrays with phase shifters at every element and time delay at each subarray input. The patterns at center frequency are shown at left. These patterns include the basic subarray pattern shown in the top figure, the array factor for the widely spaced subarrays at the center, and at the bottom the array radiation pattern, which is the product of subarray and array factor. At center frequency the array factor is shown scanned to $u = 0.5$ (30 degrees) and because of the 4 wavelength spacing between rectangular subarrays, there are grating lobes at $0.5 + p(0.25)$ for $p = \pm 1$ and -2. Fortunately these locations exactly correspond to the nulls of the subaray pattern (top), and the envelope of the array radiation pattern, the periodic sinc function at bottom left, is a smooth monotonic function.

At a higher frequency $f = 1.5f_o$, the time delay has kept the main beam of the array factor at the desired scan angle,

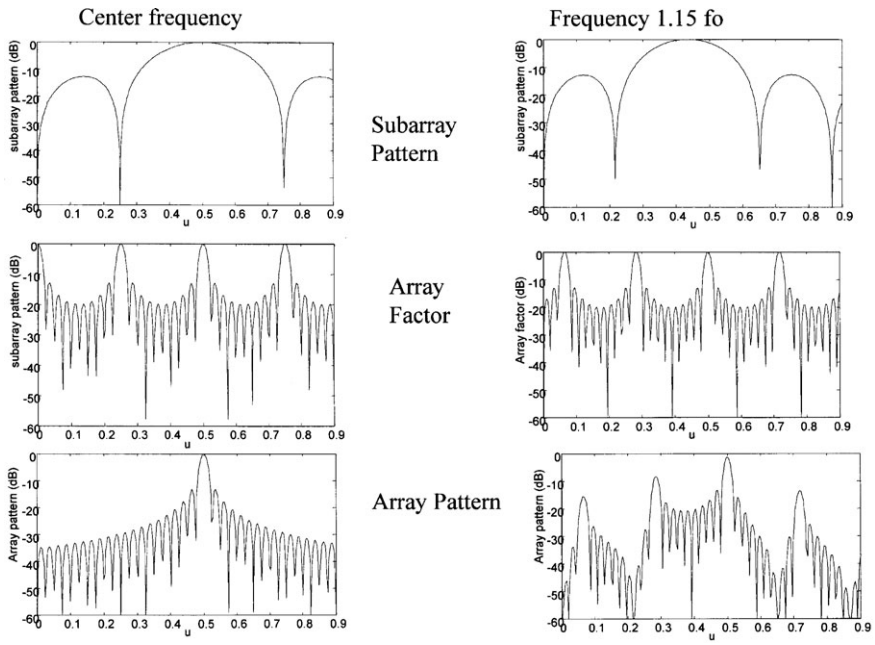

Figure 14. Subarray patterns, array factors and radiation patterns of time delay steered array at $u = 0.5$ (scanned to 30 degrees).

but now the subarray separation is effectively 4.6 lambda, and so the grating lobes are closer together. These data are shown at the right of Figure 14. More importantly, the subarray pattern, which is phase shifted, squints toward broadside so that it's peak is at $\frac{f_0}{f}\,u_0$ (approximately 0.435 instead of 0.5). The nulls are no longer aligned with the peaks of the grating lobes, and the product of subarray and array factor produces large quantization lobes.

There are several ways to reduce or eliminate these quantization lobes. Since they are caused by the periodic errors that result from quantizing the aperture phase, using an aperiodic array of subarrays instead of a fully periodic one would eliminate the quantization lobes and leave a spatial pattern with a distribution of higher average sidelobes. This approach results in improved patterns, but a loss of pattern gain because the array aperture is not completely filled. Recent studies [14] have shown that using irregular subarrays can result in a significant reduction of the quantization lobes without sacrificing aperture efficiency.

The classic method of eliminating the subarray quantization lobes is to produce a subarray pattern unlike the sinc function of Figure 14, but instead one with a pulse shape chosen so that the main beam would be within the subarray pattern envelope for all frequencies within the band Δf, but the quantization lobes outside of the pulse shaped pattern would be suppressed.

For an array with subarrays spaced D_x apart, and assuming a very large array so that the array beamwidth is much less than the subarray beamwidth, the idealized subarray pattern is shown in Figure 15 as a pulse (in u-space) with its center at the scan angle u_0, and pass band from $u_0 - \frac{0.5\,\lambda_{\min}}{D_x}$ to $u_0 + \frac{0.5\,\lambda_{\min}}{D_x}$, a width of $\Delta u = \frac{\lambda_{\min}}{D_x}$.

With a subarray pattern of this width, scanned to u_0, the nearest quantization lobes would be at $u = u_0 = -\lambda_{\min}/D_x$ and would be outside of the subarray pattern for all scan

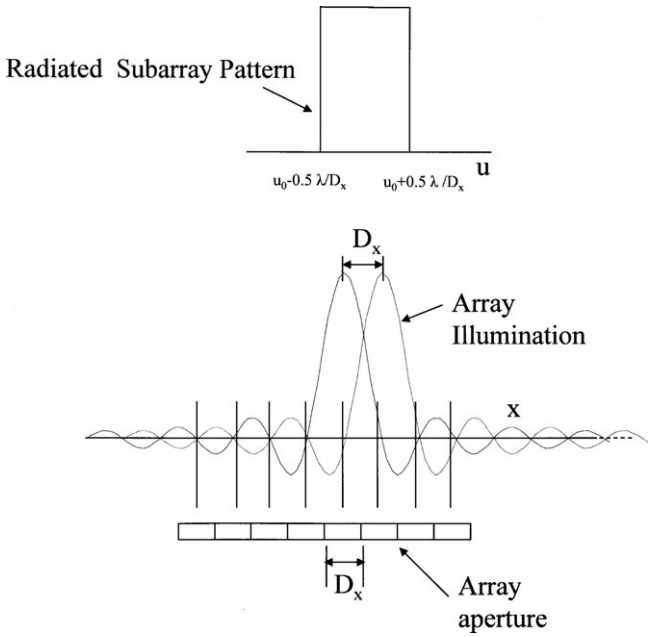

Figure 15. Ideal subarray pattern for time delay steered arrays.

angles u_0. The accompanying bandwidth is given by equation 9.

There are several ways to synthesize this type of subarray pattern, depending upon the desired bandwidth. Since the flat-topped type subarray pattern is a pulse function, the feed illumination to produce that radiation must be a sinc function that spans the whole array. Figure 15 shows that this required illlunination for each subarray overlaps all the other subarray illuminations (only two shown for clarity).

Approximations to this ideal subarray excitation have been invented by a number of authors including Mailloux [15], Dufort [16] and others. Most recently Skobelev [17]

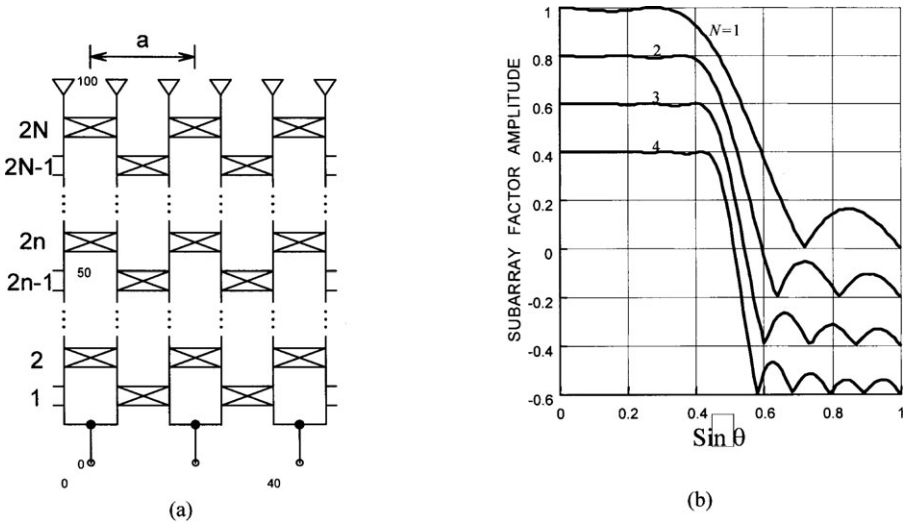

Figure 16. Chess network of Skobelev [17] (a) N-cascade (chess) network (b) Pattern of networks with N cascades for N = 1,2,3,4 (curves displaced for legibility)

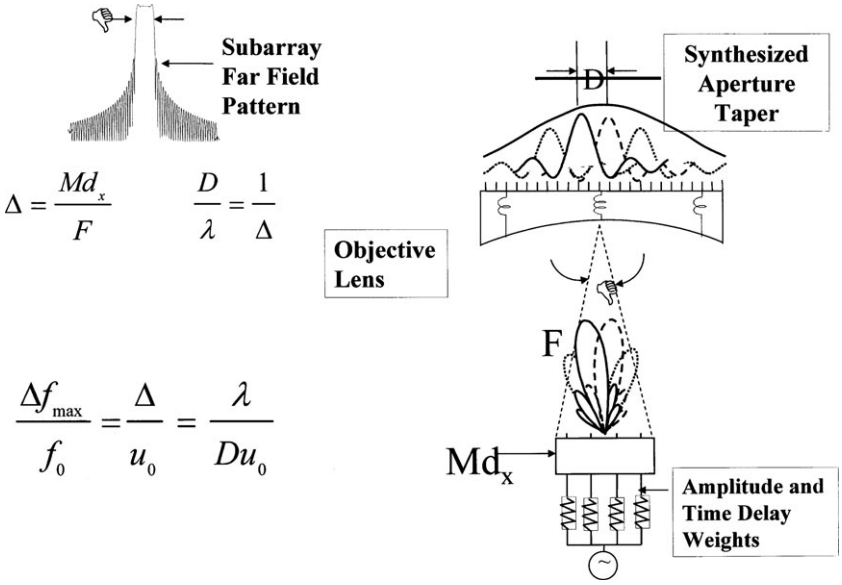

Figure 17. Overlapped subarray characteristics for lens-fed time delayed system.

has published a constrained overlapped system that offers detailed control of sidelobe levels. This network, shown schematically in Figure 16 is designed with cells of two elements each, spaced a distance "a" apart. Adjacent subarrays are therefore two elements apart. The network is called a chess-network and consists of 2N layers, or N cascades. At each cascade "N", the signals are distributed over a wider aperture, covering 2N+1 cells. As the aperture distribution becomes wider and a better approximation to a sinc function, the resulting subarray radiation pattern becomes more like a pulse function with sharper skirts and a flatter passband.

The inter-subarray spacing for these types of constrained subarrays is necessarily limited to being rather small, because large subarrays with many elements would require extremely complex, and therefore lossy, circuits. Thus, constrained subarrays are ideal for the wideband waveforms that accompany small inter-subarray spacings.

At the other extreme, for very large arrays, perhaps tens to hundreds of thousands of elements, the squint bandwidth may only be a percent or so, and then it is important to use subarrays with spacing as large as possible to reduce the number of time delays to some affordable number while increasing the bandwidth to a size appropriate to the radar or communication system. For such tasks completely overlapped subarrays can be produced by quasi-optical beamformers as shown in Figure 17. This kind of beamformer was first introduced as the Hughes Corporation HIPSAF (High Performance Scanning Array Feed) [18] and comprised of an objective lens fed by a multiple beam feed. The feed shown in the lower portion of the figure is a small multiple beam lens or a Butler matrix, or may very likely be a small digitally beamformed array. Any input to the multiple beam feed produces a linear progressive phase at its output, and this feed radiates to the back face of the objective. Two such ports are shown excited, and result in radiation patterns shown solid and dashed in the figure. Each feed produces an approximate sinc function of excitation across the main lens radiating aperture, and so each radiates like a pulse function in space.

Figure 17 also shows some of the geometric constraints and illustrates that for an equal path lens aperture, the subarray pattern width Δ is equal to the angle subtended by the feed array and that the beamwidth $\Delta f/f_0$ is given by Δ/u_0 as in equation 9. Thus, for an array with M elements spaced d_x apart, the subarray pattern width Δ is given by the objective lens size Md_x, divided by the focal length F. When all of the input ports are excited with a low sidelobe weight distribution the radiating pattern can have a low sidelobe radiation over the chosen bandwidth.

These subarray techniques have been developed to reduce system weight and the number of costly time delay components. Since they reduce the number of time delays, they are highly compatable with digital beamforming technology.

BIBLIOGRAPHY

1. W. E. Hord Microwave and millimeter wave ferrite phase shifters, *Microwave Journal State of the Art Reference*, **32**: (September) 1989.
2. A. K. Sharma Solid state control devices: State of the art, *Microwave Journal State of the Art Reference*, **32**: (September) 1989.
3. C. P. Wu Analysis of finite parallel plate waveguide arrays, *IEEE Trans. Antennas Propag.*, **AP-18** (3): 328–334, 1970.
4. P. M. Woodward A method of calculating the field over a plane aperture required to produce a given polar diagram, *Proc. IEE (London), Part 3A*, **93**: 1554–1555, 1947.
5. J. Butler R. Loe Beamforming matrix simplifies design of electronically scanned antennas, *Electronic Design*, **9**: 170–173, (12 April) 1961.
6. S. A. Schelkunov A mathematical theory of linear arrays, *Bell System Tech J.*, 80–107, 1943.
7. C. L. Dolph A current distribution for broadside arrays which optimizes the relationship between beamwidth and sidelobe level, *Proc. IRE*, **34**(June): 335–345, 1946.
8. T. T. Taylor Design of line source antennas for narrow beamwidth and low sidelobes, *IEEE Trans. Antennas Propag.*, **AP-3**: 16–28, (January) 1955.
9. E. T. Bayliss Design of monopulse antenna difference patterns with low sidelobes, *Bell System Tech. J.*, **47**: 623–640.
10. R. S. Elliott On discretizing continuous aperture distributions, *IEEE Trans. Antennas Propag.*, **AP-25**: 617–621, (September) 1977.
11. H. R. Orchard R. S. Elliott G. J. Stern Optimizing the synthesis of shaped antenna patterns, *IEE Proc. (London) Part H* **(1)**: 63–66, 1984.
12. F. Ares *et al*. Application of genetic algorithms and simulated annealing technique in optimising the aperture distributions of antenna array patterns, *Electronic Lett.*, **32** (3): 148–149, 1996.
13. M. K. Skolnik J. W. Sherman III F. C. Ogg, Jr. Statistically Designed Density-Tapered Arrays, *IEEE Trans. Antennas Propag.*, **AP-12**: 408–417, (July) 1964.
14. R. J. Mailloux, S. G. Santorelli and T. M. Roberts," Wideband Arrays using Irrregular (Polyomino) shaped Subarrays", *electronics Letters*, Vol.**42**, No.18,Aug. 2006, pp. 1019–1020
15. R. J. Mailloux," An Overlapped Subarray for Limited Scan Applications", *IEEE Trans*. **AP-22**, No.3,May 1974, pp. 487–489
16. E. C. Dufort," Constrained feeds for limited scan arrays", *IEEE Trans.* **AP-26**,May 1978, pp. 407–413
17. S. P. Skobelev," Methods of constructing optimum phased-array antennas for limited field of view", *IEEE Antennas and Propagation Magazine*, Vol. **40**, No.2,April 1998, pp. 39–49
18. R. Tang," Survey of Time-Delay Steering Techniques," *Phased Array Antennas*, pp. 254–260, Artech House, Dedham, MA, 1972

ROBERT J. MAILLOUX
University of Massachusetts,
Dept. of Electrical and
Computer Engineering,
Amherst, MA